Formation and Characterization of Titania Nanosheet-Precipitated Coatings via Sol−Gel Process with Hot Water Treatment under Vibration

Atsunori Matsuda,*,† Tatsuo Matoda,‡ Toshihiro Kogure,§ Kiyoharu Tadanaga,‡ Tsutomu Minami,‡ and Masahiro Tatsumisago‡

Department of Materials Science, Toyohashi University of Technology, 1-1 Hibarigaoka, Tempaku-cho, Toyohashi, Aichi 441-8580, Japan, Department of Applied Materials Science, Graduate School of Engineering, Osaka Prefecture University, Sakai, Osaka 599-531, Japan, and Department of Earth and Planetary Sciences, Graduate School of Science, The University of Tokyo, 7-3-1 Hongo, Bunkyo-ku, Tokyo 113-0033, Japan

Received October 25, 2004. Revised Manuscript Received December 6, 2004

Vibrations were found to affect the nanostructure of titania crystallites formed on SiO_2-TiO_2 gel coatings during hot water treatment. Granular anatase nanocrystals of 30−50 nm in size were formed on the coatings during hot water treatment without vibration, whereas the shape of the precipitates elongated to be sheetlike by applying a vibration to the substrate during hot water treatment. The sheetlike crystals mainly consisted of nanosheets with a spacing of about 0.6 nm, and were identified as a hydrated titania, $m(TiO_2)\cdot nH_2O$, with the lepidocrocite-like layered structure. Titania nanosheets were characterized by a large surface-to-volume ratio, allowing the high photocatalytic reactivity comparable to that of anatase crystals. In addition, the coatings were highly transparent even after the formation of the nanosheets and thermally stable at around 500 °C. The hydrated titania nanosheet-precipitated coatings maintained an excellent wettability for water and antifogging properties even after being kept in dark for 2000 h due to their unique physicochemical properties. Processing temperatures for the coatings preparation are lower than 100 °C under atmospheric pressure, so that the coatings have a great potential for applications to various substrates including organic polymers with poor heat resistance.

Introduction

Nanocrystal-dispersed materials such as bioactive glass-ceramics, ferromagnetic alloys, and photofunctional inorganic−organic composites have created an important field in science and technology because of their exceptional chemical and physical properties.[1−4] The characteristics of nanocrystal-dispersed materials basically depend on the properties of the dispersed crystallites in nanometer size and the residual phase which makes up the materials. On the other hand, in the weathering process of minerals, dissolution of specific components, ion exchange, and diffusion of molecular water into the materials occur, resulting in the formation of nanocrystals on the surface or in the bulk of residual materials.[5] Thus, the weathering can be regarded as a natural and eco-friendly way to obtain nanocrystal-dispersed materials. However, it takes an extraordinarily long period, i.e., geological time, to obtain such materials during natural weathering at an ambient temperature and under atmospheric pressure, mainly due to the low solubility of the components and low diffusion rate of water molecules.

Inorganic gel materials prepared by the so-called "sol−gel method" using metal alkoxides as starting materials are generally porous and have a large specific surface area, so that the gel materials can easily react with water vapor and/or water liquid in a much shorter time.[6−8] In the case of multicomponent inorganic gel materials, hetero-bondings such as M−O−M′ (M and M′, metals; O, oxygen), which are often not stable from a thermodynamic point of view, are readily hydrolyzed, and specific components dissolve and recrystallize in water. For instance, we have shown that anatase nanocrystals were formed on sol−gel derived SiO_2-TiO_2 coatings with water vapor or hot water treatments.[7,9,10] Anatase formation proceeds through hydrolysis of Si−O−Ti bonds, dissolution of SiO_2 component, migration of hydrolyzed titania species, and nucleation and growth of

* Corresponding author. E-mail: matsuda@tutms.tut.ac.jp.
† Toyohashi University of Technology.
‡ Osaka Prefecture University.
§ The University of Tokyo.

(1) Strnad, Z. *Glass−Ceramics Materials*. Glass Science and Technology Series, Vol. 8; Elsevier Science: New York, 1986.
(2) Masumoto, T. Recent Progress in Amorphous Metallic Materials in Japan. In *Materials Science and Engineering: A, Structural Materials: Properties, Microstructure and Processing*; Elsevier Science: New York, 1994.
(3) Kagan, C. R.; Mitzi, D. B.; Dimitrakopoulos, C. D. *Science* **1999**, *286*, 945.
(4) Hagfeldt, A.; Gratzel, M. *Chem. Rev.* **1995**, *95*, 49.
(5) Doremus, R. H. *Glass Science*; John Wiley & Sons: New York, 1994.
(6) Matsuda, A.; Kogure, T.; Matsuno, Y.; Katayama, S.; Tsuno, T.; Tohge, N.; Minami, T. *J. Am. Ceram. Soc.* **1993**, *76*, 2899.
(7) Matsuda, A.; Kogure, T.; Matsuno, Y.; Katayama, S.; Tsuno, T.; Tohge, N.; Minami, T. *J. Ceram. Soc. Jpn.* **1994**, *102*, 330.
(8) Imai, H.; Morimoto, H.; Tominaga, A.; Hirashima, H. *J. Sol-Gel Sci. Technol.* **1997**, *10*, 45.
(9) Matsuda, A.; Kotani, Y.; Kogure, T.; Tatsumisago, M.; Minami, T. *J. Am. Ceram. Soc.* **2000**, *83*, 229.
(10) Kotani, Y.; Matsuda, A.; Kogure, T.; Tatsumisago, M.; Minami, T. *Chem. Mater.* **2001**, *13*, 2144.

10.1021/cm048135h CCC: $30.25
Published on Web 01/29/2005

TiO_2. The hydrolysis, dissolution, and recrystallization are influenced not only by the physicochemical conditions such as temperature, pressure, and pH of the solution but also by external dynamic conditions such as the vibration of the materials and the flow of the solution. Thus, these reactions of the gel materials with water under external dynamic conditions should influence the nucleation, growth, and characteristics of the nanocrystals. With respect to titania-based nanomaterials, much attention is being devoted to their practical applications such as photocatalysts to decompose environmental pollutants[11] and photoinduced superhydrophilicity[12−14] as attested by the increasing number of research reports in this field.[15] In addition, the control of their nanostructures based on the orientation and growth of titania nanocrystals offers an exciting opportunity for developing a new class of materials with unique physical and chemical properties.[16−19]

Here we report the formation and detailed characterization of unusual titania nanosheet-precipitated coatings on substrates from sol−gel derived SiO_2-TiO_2 films through hot water treatment under vibration. Nanosheets are characterized by a large surface-to-volume ratio, allowing high reactivity at the nanosized level. The titania nanosheets in this study mainly consist of several hydrated titania layers with a spacing of about 0.6 nm. The coatings of hydrated titania show high photocatalytic activities, lasting excellent hydrophilicity, and antifogging properties due to their unique physicochemical properties. The preparation of the titania nanosheet-precipitated coatings has been achieved by a new finding that vibrations during hot water treatment affect significantly the nanostructure of the formed titania.

Experimental Section

Preparation of Coatings. SiO_2-TiO_2 sols containing 25 mol % TiO_2 were prepared from the corresponding metal alkoxides. Silicon tetraethoxide (Wako Pure Chemical Industry) in ethanol was hydrolyzed with water containing 3.6 mass % HCl at room temperature for 30 min; the mole ratios of ethanol and water to silicon tetraethoxide were 5 and 4, respectively. The hydrolyzed solution was then mixed with titanium tetra-*n*-butoxide (Wako Pure Chemical Industry) diluted with ethanol and stirred for 30 min. The mole ratio of ethanol to titanium tetra-*n*-butoxide was 20. The SiO_2-TiO_2 coatings were fabricated on nonalkali glass plates (NA35, NH Techno Glass), silica glass plates (Sumikin Ceramics & Quartz), and silicon wafers (Mitsubishi Sumitomo Silicon) by a dipping−withdrawing method at a rate of about 3.0 mm s^{-1}. The coating process was carried out in an ambient atmosphere at room temperature. The substrates with coatings were dried at 90 °C for 60 min in air using an oven and then immersed into 300 mL of hot water at 90 °C under vibration of 0 to 25 Hz with amplitude of 2.5 mm. A handmade apparatus consisting of a clip shaft, a transducer, a variable resistor, and a direct-current power source was used for applying a given vibration to the substrate.

The changes in the texture of the coatings during hot water treatment were examined using a field-emission type scanning electron microscope (FE-SEM, model S-4500, Hitachi). The structures of the coatings and precipitates were identified by using a field-emission type transmission electron microscope (FE-TEM, model HF-2000, Hitachi), equipped with an energy-dispersive X-ray spectrometer (EDS, Sigma, Kevex). Electron-transparent specimens for the TEM examination were prepared by using an Ar ion-milling. The thermal stability and phase transition of coatings were also examined on SEM and TEM. Average roughness and profile of the coatings were evaluated using an atomic force microscope (AFM, Nanopics, Seko Instruments). The thickness of the coatings was evaluated using a surface profilometer (TDA-22, Kosaka Laboratory).

Characterization of Coatings. Fourier-transformed infrared (FTIR) absorption spectra of the coatings on silicon substrates were measured in transmission mode using an FT-IR spectrophotometer (FT-IR1650, Perkin-Elmer). Chemical analyses for the composition of the coatings were carried out with X-ray photoelectron spectroscopy (ESCA-K1, Shimadzu). Ultra violet−visible (UV−Vis) transmission spectra of silica glass or nonalkali glass substrates of which one side was coated with a film were obtained using a UV−Vis spectrophotometer (V-560, JASCO). The pencil hardness and adhesion strength of the coatings to the substrates were examined according to JIS-K-5400.

Photocatalytic bleaching of methylene blue (MB) (Wako Pure Chemical Industry) with coatings after hot water treatment with and without vibration was examined. The nonalkaline glass substrates with coatings were immersed into a Pyrex spectrophotometer cell containing 1×10^{-5} mol dm^{-3} MB aqueous solution (2.0 g), and then the cell was sealed with a silicone rubber stopper. The area of the coatings on the substrates was fixed to be 1.0 cm^2. The substrates were irradiated with UV light from the uncoated side using a super high-pressure Hg lamp (USH-250BY, Ushio Denki) for several periods of time. The light wavelength shorter than 350 nm was cut off using a color glass filter (UV-33, Asahi Techno Glass) to prevent the direct degradation of MB during the UV irradiation. The intensity of the UV light irradiated was ca. 67 mW cm^{-2}. The changes in concentrations of MB in the aqueous solution were examined from absorption spectra measured on a UV spectrophotometer (V-560, JASCO). Changes in contact angle for water of the coatings with UV light irradiation were measured using a contact angle meter (CA-C, Kyowa Surface Science).

Results and Discussion

Formation of Titania Nanosheet-Precipitated Coatings. Nonalkali glass substrates coated with $75SiO_2 \cdot 25TiO_2$ (in mol %) film were treated with hot water at 90 °C under various vibration frequencies with an amplitude of 2.5 mm. Granular precipitates of 30−50 nm in diameter, which were identified as anatase, were formed on the coatings after the hot water treatment without vibration. The shape of the

(11) (a) Mao, Y.; Schoneich, C.; Asmus, K. D. *Photocatalytic Purification of Water and Air*; Elsevier: New York, 1993; pp 49−66. (b) Yamashita, H.; Ichihashi, Y.; Anpo, M.; Hashimoto, M.; Louis, C.; Che, M. *J. Phys. Chem.* **1966**, *100*, 16041.
(12) Choy, J.; Park, J.; Yoon, J. *J. Phys. Chem B* **1998**, *102*, 5991.
(13) Papoutsi, D.; Lianos, P.; Yianoulis, P.; Koutsoukos, P. *Langmuir* **1994**, *10*, 1684.
(14) (a) Wang, R.; Hashimoto, K.; Fujishima, A.; Chikuni, N.; Kojima, E.; Kitamura, A.; Shimohigosi, M.; Watanabe, T. *Nature* **1997**, *388*, 431. (b) Wang, R.; Sasaki, N.; Fujishima, A.; Watanabe, T.; Hashimoto, K. *J. Phys. Chem. B* **1999**, *103*, 2188. (c) Machida, M.; Norimoto, K.; Watanabe, T.; Hashimoto, K..; Fujishima, A. *J. Mater. Sci.* **1999**, *34*, 2569.
(15) (a) Hoffmann, M. R.; Martin, S. T.; Choi, W.; Bahnemann, D. *Chem. Rev.* **1995**, *95*, 69. (b) Linsebiger, A. L.; Lu, G.; Yates, T., Jr. *Chem. Rev.* **1995**, *95*, 735.
(16) Tadanaga, K.; Morinaga, J.; Matsuda, A.; Minami, T. *Chem. Mater.* **2000**, *12*, 590.
(17) Grimes, C. A.; Sigh, R. S.; Dickey, E. C.; Varghese, O. K. *J. Mater. Res.* **2001**, *16*, 1686.
(18) Penn, R. L.; Banfield, J. F. *Geochim. Cosmochim. Acta* **1999**, *63*, 1549.
(19) Banfield, J. F.; Welch, S. A.; Zhang, H.; Ebert, T. T.; Penn, R. L. *Science* **2000**, *289*, 751.

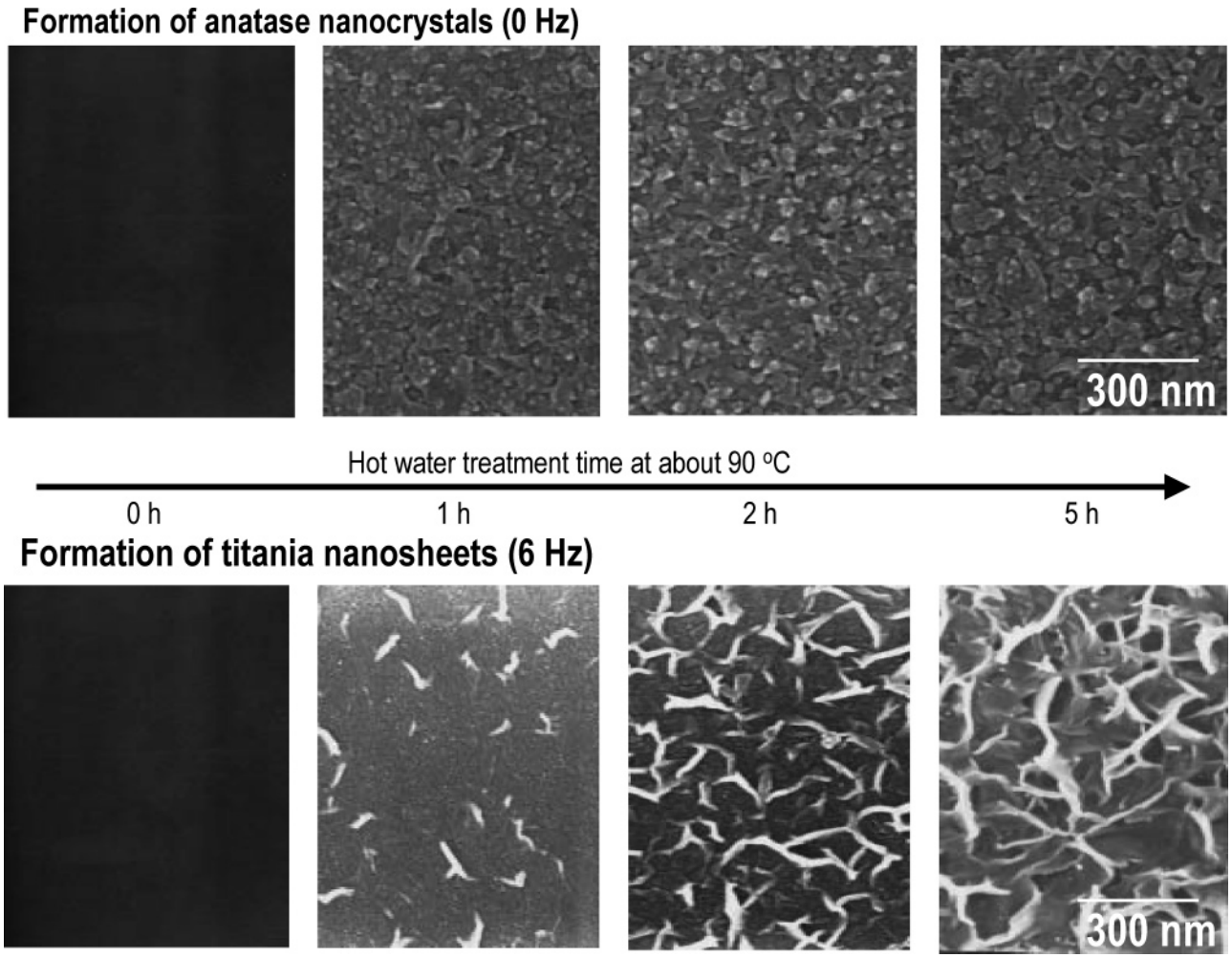

Figure 1. SEM images of the formation of granular precipitates, which were identified as anatase, without vibrations, and sheetlike precipitates with vibration at 6 Hz on SiO_2-TiO_2 coatings during hot water treatment at 90 °C.

precipitates became elongated by applying vibration to the substrate during hot water treatment. Longitudinal vibration was preferable to transverse vibration for formation of the sheetlike precipitates. When the substrates with SiO_2-TiO_2 coatings were treated with hot water under longitudinal vibration of ca. 6 Hz, the shape of the precipitates clearly became nanosheetlike. However, the amounts of the nanosheet precipitates decreased under longitudinal vibration of ca.10 Hz and almost no precipitates were formed over ca. 12.5 Hz. SEM images of the formation of granular anatase without vibration and nansheet precipitates with vibration at ca. 6 Hz during the hot water treatment are shown in Figure 1. The amount of both precipitates increased with hot water treatment, whereas the shapes and growth rates of the precipitates are clearly different. Under the vibration, nanosheet precipitates are preferentially formed at a lower growth rate on the coating during hot water treatment. Such a unique phenomenon in the formation of titania precipitates with hot water treatment in the SiO_2-TiO_2 system was not observed for the sol−gel derived pure TiO_2 coatings under the same conditions.

Changes in average roughness of the SiO_2-TiO_2 coatings during the hot water treatment without vibration and with vibration at ca. 6 Hz evaluated using AFM are shown in Figure 2. Under both conditions the surface roughness of

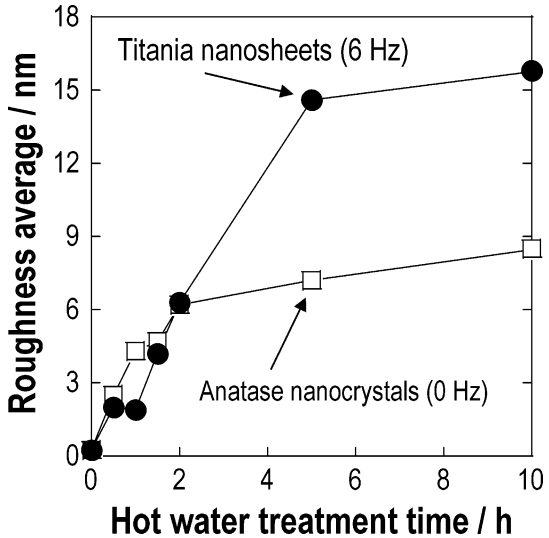

Figure 2. Changes in average roughness of the SiO_2-TiO_2 coatings during the hot water treatment without vibrations and with vibrations at ca. 6 Hz evaluated using AFM.

the coatings increases with treatment time. The value of average roughness of the coating without vibration tends to level off to be about 7 nm over 2 h, whereas that of the coating under the vibration appears to be saturated about 15 nm over 5 h. These surface roughness changes of the coatings

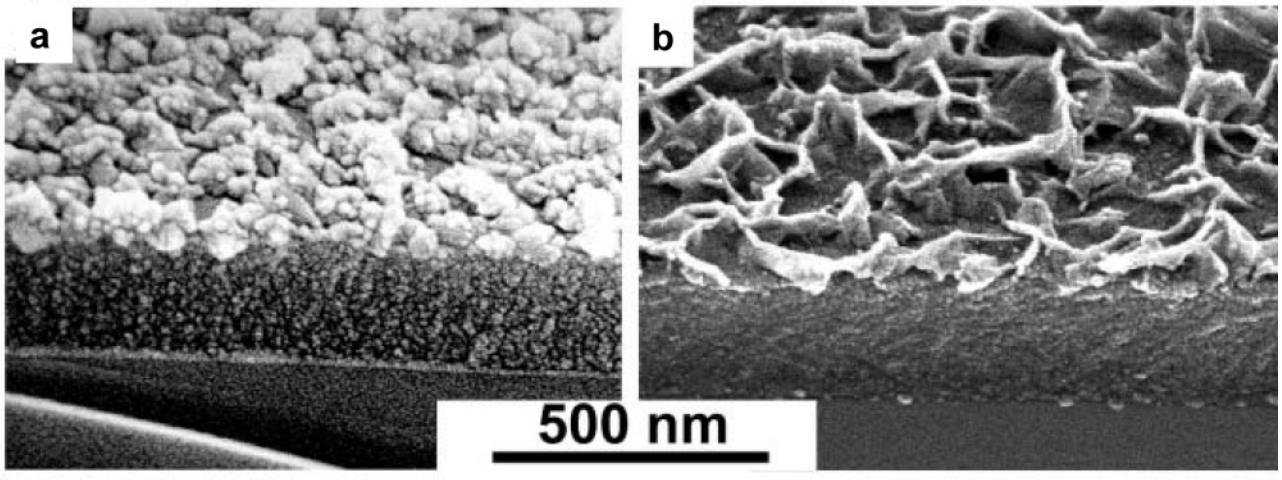

Figure 3. SEM images of (a) granular precipitates and (b) sheetlike precipitates on the coatings. Granular precipitates were obtained without vibration during hot water treatment at 90 °C for 1 h. Sheetlike precipitates were obtained under longitudinal vibrations of ca. 6 Hz during hot water treatment at 90 °C for 5 h.

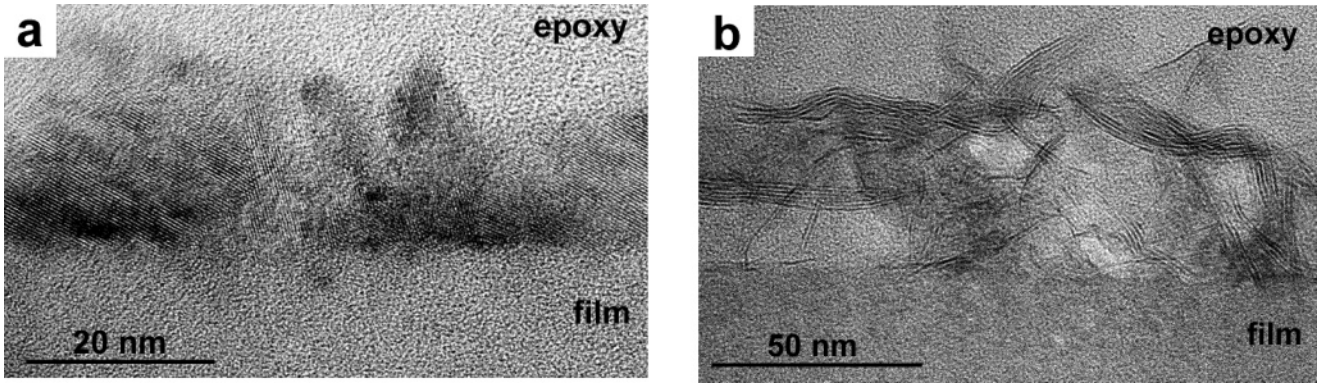

Figure 4. Cross-sectional TEM images of (a) granular precipitates and (b) sheetlike precipitates on the coatings. Preparation conditions of granular precipitates and sheetlike precipitates are the same as in Figure 3.

are corresponding to the changes in surface morphology due to the formation of precipitates shown in Figure 1.

Cross-sectional SEM and TEM images of granular precipitates and nanosheet precipitates on the coatings are compared in Figures 3 and 4, respectively. Granular precipitates were obtained without vibration during hot water treatment for 1 h. Nanosheet precipitates were obtained under longitudinal vibration of ca. 6 Hz during hot water treatment for 5 h. Granular precipitates of 30−50-nm diameter (Figure 3a) and the characteristic lattice fringes of the granular precipitates (Figure 4a) are observed. The granular precipitates were composed of the nanocrystals with lattice fringes of 0.35-nm spacing, which corresponded to the d-value of (101) in anatase as reported in previous papers.[9,10] On the other hand, nanosheet precipitates of about 100 nm (Figure 3b) and the characteristic lattice fringes of the nanosheet with layered structure (Figure 4b) are seen. According to the SEM and TEM images, the nanosheets seem to be oriented at angles with the substrate. Fourier analysis of the TEM image suggested that the nanosheet precipitates consisted of layers with a spacing of about 0.6 nm; the spacing of 0.6 nm was not found in any pure TiO_2 crystalline phases reported previously, such as anatase, rutile, and brookite. The underlayers of anatase nanocrystals and titania nanosheets were amorphous.

EDS of the nanosheet precipitates and the underlayer was acquired from the cross-sectional TEM specimen in Figure 4b by using a nanosized electron probe. Silicon, titanium, and oxygen are detected from the underlayer, whereas silicon is hardly detected in the nanosheets taking into account the contamination from the surrounding area. Therefore, the nanosheets precipitated mainly consist of titanium and oxygen.

For the precise identification of the titania nanosheets, plan-view TEM specimens were prepared to obtain high-resolution images (HRTEM) and significant electron diffractions by ion-milling the substrate from the backside. The HRTEM images of the titania nanosheets are shown in Figure 5a and b. The titania nanosheets were found to basically consist of layers with a spacing of 0.6−0.63 nm (Figure 5a) and include layers with a spacing of around 0.8 nm (Figure 5b). An electron diffraction pattern from the plan-view TEM specimen of the nanosheet-precipitated coatings is shown at the bottom of Figure 6. A pattern from anatase nanocrystal-precipitated coatings obtained without vibration and Debye−Scherrer rings calculated for anatase are shown at the top-right in Figure 6 for comparison. The observed diffraction pattern from the anatase nanocrystals obtained without vibration agrees well with the calculated one. On the other hand, the pattern from the nanosheets, which is characterized with three distinctive Deby-Scherrer rings corresponding to

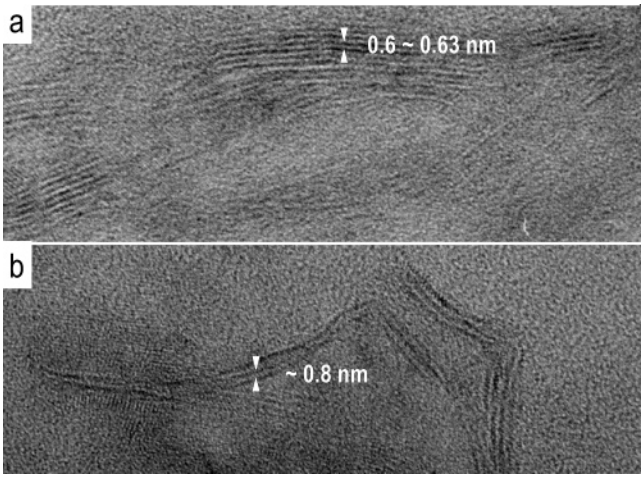

Figure 5. High-resolution TEM images of the titania nanosheets. The nanosheets consist of layers with a spacing of 0.6−0.63 nm (a) and include layers with a spacing of around 0.8 nm (b).

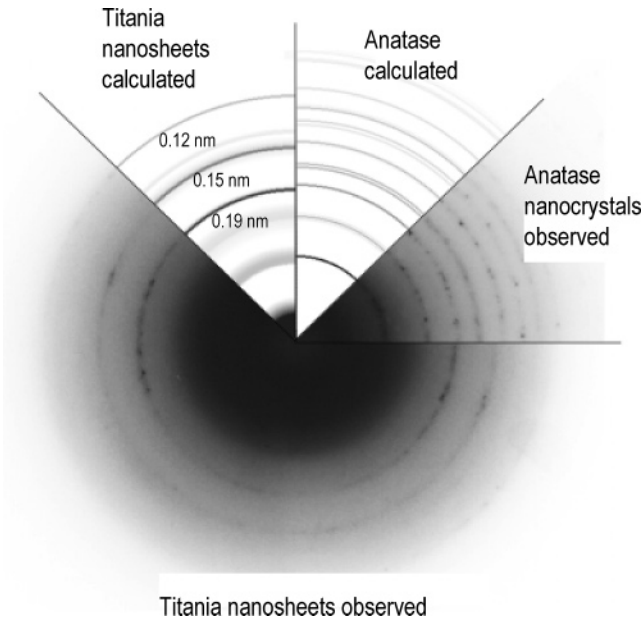

Figure 6. Electron diffraction pattern from the titania nanosheets obtained with longitudinal vibrations of ca. 6 Hz (bottom). Diffraction pattern from the antase nanocrystals obtained without vibrations (right). The calculated pattern, Debye−Scherrer rings, for anatase is also shown for comparison (top right). The calculated pattern for the randomly oriented monolayers of hydrated titania with the lepidocrocite-like structure (top left).

0.19, 0.15, and 0.12 nm, is thoroughly different from that of anatase, indicating that a different crystalline phase is formed. Recently Sasaki et al. reported a hydrated titania nanosheet with a lepidocrocite-like layered structure.[20,21] We have calculated the diffraction pattern from randomly oriented monolayers with this lepidocrocite-like structure using the Debye equation.[22] The result is shown at the top left in Figure 6. The three Debye−Scherrer rings in the observed pattern from the nanosheets are well reproduced. From this result, we conclude that the nanosheet found in the present study

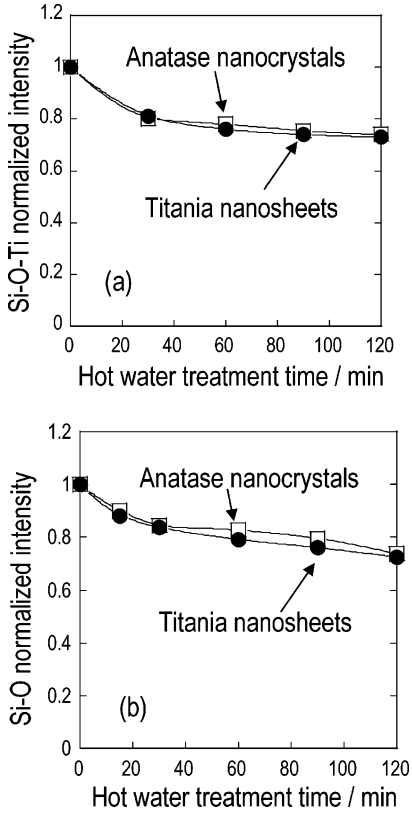

Figure 7. Variations in the absorption bands at 950 cm^{-1} due to Si−O−Ti bonds (a) and at around 1100 cm^{-1} assigned to Si−O bonds (b) during hot water treatment for SiO_2−TiO_2 coatings without vibration (open squares) and under vibration at 6 Hz (closed circles).

basically consists of the hydrated titania like $m(TiO_2)\cdot nH_2O$ with the lepidocrocite-like layered structure. It is still not clear whether these layers are orderly stacked or turbostratic in the nanosheet.

It has been reported that hydrated titania with a spacing between 0.6 and 0.9 nm can be prepared by ion exchange between protons and alkali ions in alkali titanate such as $Na_2Ti_3O_7$, $K_2Ti_4O_9$, or $Cs_2Ti_5O_{11}$, which were obtained by a flux method at high temperatures around 1000 °C using titanium dioxide and the corresponding alkali carbonate.[23−27] With respect to hydrated titania nanosheets, Sasaki et al. reported the synthesis of the nanosheets through exfoliation and delamination of hydrated titania flakes obtained with the ion exchange.[25] However, hydrated titania nanosheet-precipitated coatings in the present study have a unique surface topography. We emphasize that this type of unique coatings with the nanosheet-precipitates could not be obtained through conventional sol−gel processes on the basis of the heat treatment of gel coatings from the sols.

Formation Mechanism of Titania Nanosheets. In the preceding papers,[9,10] we have proposed that anatase nanocrystals were formed on SiO_2−TiO_2 coatings with hot water

(20) Sasaki, T.; Watanabe, M.; Michiue, Y.; Komatsu, Y.; Izumi, F.; Takenouchi, S. *Chem. Mater.* **1995**, *7*, 1001.
(21) Sasaki, T.; Ebina, Y.; Kitami, Y.; Watanabe, M.; Oikawa, T. *J. Phys. Chem. B* **2001**, *105*, 6116.
(22) Waychunas, G. A. Structure, Aggregation and Characterization of Nanoparticles. In *Reviews in Mineralogy and Geochemistry*, Vol. 44; Mineralogical Society of America: Washington, DC, 2001.
(23) Sasaki, T.; Komatsu, Y.; Fujiki, Y. *Chem. Mater.* **1992**, *4*, 894.
(24) Feist, T. P.; Davis, P. K. *J. Solid State Chem.* **1992**, *101*, 275.
(25) (a) Sasaki, T.; Nakano, S.; Yamauchi, S.; Watanabe, M. *Chem. Mater.* **1997**, *9*, 602. (b) Sasaki, T.; Ebina, Y.; Tanaka, T.; Harada, M.; Watanabe, M.; Decher, G. *Chem. Mater.* **2001**, *13*, 4661.
(26) Yin, S.; Uchida, S.; Fujishiro, Y.; Aki, M.; Sato, T. *J. Mater. Chem.* **1999**, *9*, 1191.
(27) Yanagisawa, M.; Uchida, S.; Yin, S.; Sato, T. *Chem. Mater.* **2001**, *13*, 174.

treatment as follows: (i) hydrolysis of Si−O−Ti bonds and dissolution of the SiO_2 component; (ii) migration of hydrolyzed titania species from inside to surface of the coating; and (iii) nucleation and growth of anatase nanocrystals at the surface of the residual coating. The effects of the vibration on the structural changes in the SiO_2−TiO_2 coatings during hot water treatment were investigated from IR absorption spectra. The intensities of the absorption bands at 950 cm^{-1} due to Si−O−Ti bonds[28] and at around 1100 cm^{-1} assigned to Si−O bonds[29] were decreased, whereas the positions of the bands were hardly changed. Variations in the intensity of these bands due to Si−O−Ti and Si−O bonds are shown in Figure 7a and b**,** respectively. Open squares and closed circles represent the coatings without vibration and with a vibration at ca. 6Hz, respectively. It can be seen that the vibration during hot water treatment accelerates neither hydrolysis of Si−O−Ti bonds nor dissolution of SiO_2 component. The normalized intensities of the bands due to Si−O−Ti and Si−O bonds decrease to be about 0.7 in 120 min during the hot water treatment, which is independent of the vibrations. Therefore, the formation of anatase nanoparticles and titania nanosheets is dominated not by the hydrolysis of Si−O−Ti bonds or dissolution of SiO_2 component but by nucleation and growth of hydrolyzed titania species at the surface of the coating. Rapid water flow driven by vibrations probably increases the collision rate between gel coating and water molecules, and lowers the surface concentration of hydrolyzed titania species. This facilitates the formation of nanocrystals including proton, hydroxyl, and oxonium ion in the structure, which should prevent the formation of anatase or the transformation from hydrated titanate to anatase, and to allow growth of hydrated titanate to form nanosheets. On the other hand, it was found that granular anatase precipitates were formed on the SiO_2−TiO_2 coatings containing different amounts of TiO_2, i.e. 9, 16.5, and 33 mol %, during hot water treatment without vibration. Thus the increase in interaction between hydrolyzed titania species and water due to the vibration is considered to have a greater influence on the formation of titania nanosheets than the chemical composition of the coatings. These phenomena demonstrate that the crystalline phase and the morphology of nanocrystal-dispersed materials can be controlled by treating sol−gel derived multicomponent gels with hot water under external dynamic conditions such as vibrations.

The atomic percent of titanium and oxygen, and the atomic ratio of titanium to oxygen of anatase nanocrystals and titania nanosheets precipitated on the SiO_2−TiO_2 coatings after hot water treatment, have been investigated using X-ray photoelectron spectroscopy (XPS). Those of pure TiO_2 (anatase) coating obtained from titanium tetra-*n*-butoxide with heat treatment at 500 °C have been also examined for comparison. These results are summarized in Table 1.

XPS revealed that the titanium to oxygen atomic ratio of nanosheets obtained with vibrations was larger than those of anatase nanocrystals obtained without vibration and of pure TiO_2 (anatase) obtained at 500 °C. In addition, the binding energies of Ti2p and O1s bands in the hot water treated anatase nanocrystals, titania nanosheets, and thermally treated pure TiO_2 (anatase) are shown in Table 2. The binging energies of Ti2p bands are almost the same (458.2−458.3 eV) which is reported for pure TiO_2,[30] whereas the binding energy of O1s band (530.1 eV) for nanosheets is larger than those of thermally treated TiO_2 (anatase) and anatase nanocrystals. The O1s band with a larger binding energy is associated with hydroxyl groups.[30] These results in XPS measurements supporting the fact that the nanosheet was identified as hydrated titani-like $m(TiO_2)\cdot nH_2O$ with the lepidocrocite-like layered structure which is originated from a significant interaction between hydrolyzed titania species and water molecules.

Table 1. Atomic Percent of Ti and O, and Atomic Ratio of O/Ti in TiO_2(anatase) Coating Obtained by Heat Treatment at 500 °C, Anatase Nanocrystal- and Titania Nanosheet-Precipitated SiO_2−TiO_2 Coatings after Hot Water Treatment

	Ti (at. %)	O (at. %)	O/Ti
TiO_2(anatase)	28.2	71.8	2.54
anatase nanocrystal-precipitated SiO_2−TiO_2 coating	25.3	74.7	2.96
titania nanosheet-precipitated SiO_2−TiO_2 coating	23.4	76.7	3.28

Table 2. Binding Energy of Ti2p and O1s Peaks in TiO_2(anatase) Coating Obtained by Heat Treatment at 500 °C, Anatase Nanocrystal- and Titania Nanosheet-Precipitated SiO_2−TiO_2 Coatings after Hot Water Treatment

	binding energy (eV)	
	Ti2p	O1s
TiO_2(anatase)	458.3	529.5
anatase nanocrystal-precipitated SiO_2−TiO_2 coating	458.3	529.7
titania nanosheet-precipitated SiO_2−TiO_2 coating	458.2	530.1

Characterization of Coating Properties. Optical transmittance of anatase- and hydrated titania nanosheet-precititated coatings on silica glass substrates was as high as about 90% in the visible range including Fresnel's reflectance, indicating that the anatase nanocrystals and hydrated titania nanosheets cause no light scattering. Absorption edge was estimated to be about 360 nm for both coatings. Interference wavy patterns were very small, so that the refractive index of the coatings almost matched with that of the silica glass substrate due to large porosity at the surface of the coating and the presence of a silica-rich underlayer.

Pencil hardness of the SiO_2−TiO_2 coating was less than 2B before hot water treatment and increased during the treatment owing to the formation of nanocrystals and the densification of the coating. Anatase nanocrystal-precipitated coatings obtained with a hot water treatment at 90 °C for 1 h showed pencil hardness of HB−H, whereas that of hydrated titania nanosheet-precipitated coatings obtained with a hot water treatment at 90 °C for 5 h under vibrations was B−HB. Lower pencil hardness of the latter can be ascribed to the higher roughness due to hydrated titania nanosheets on the coating.

(28) (a) Mukherjee, S. P. *J. Non-Cryst. Solids* **1980**, *42*, 477. (b) Ricchiardi, G.; Damin, A.; Bordiga, S.; Lamberti, C.; Spano, G.; Rivetti, F.; Zecchina, *J. Am. Ceram. Soc*. **2001**, *123*, 11409.
(29) Morikawa, H.; Osuka, T.; Marumo, F.; Yasumori, A.; Yamane, M. *J. Non-Cryst. Solids* **1986**, *82*, 97.
(30) Yu, J.; Zhao, X. *Mater. Res. Bull*. **2001**, *36*, 97.

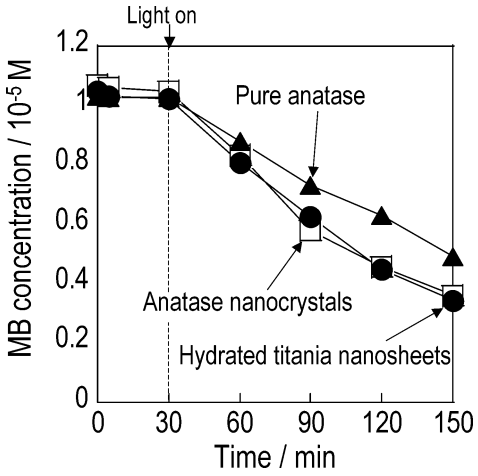

Figure 8. Changes in the concentration of MB as a photocatalytic reactant in aqueous solutions in the optical cells containing the glass substrates with coatings during UV light irradiation. Open squares are for anatase nanocrystals-precipitated coating and closed circles are for hydrated titania nanosheet-precipited coating. Closed triangles are for pure anatase coating prepared from alkoxide-derived gel film by heat treatment at 500 °C for comparison.

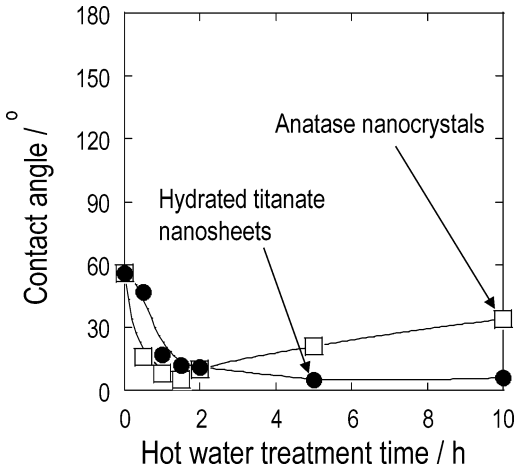

Figure 9. Changes in contact angles for water of SiO_2-TiO_2 coatings during hot water treatment. Open squares and closed circles represent the treatment conditions for anatase formation without vibration and for hydrated titania formation with vibrations at ca. 6 Hz, respectively.

Photocatalytic activities of the coatings were evaluated from changes in the concentration of MB as a photocatalytic reactant in aqueous solutions during UV light irradiation (Figure 9). Open squares are for anatase nanocrystal-precipitated coatings obtained by the hot water treatment at 90 °C for 1 h without vibration, and closed circles are for hydrated titania nanosheet-precipited coatings obtained by the hot water treatment at 90 °C for 5 h under ca. 6 Hz vibration. Closed triangles are for pure TiO_2 anatase coating prepared by heat treatment at 500 °C for comparison. The concentration of MB for all the coatings is almost constant before UV irradiation, indicating that the adsorption effect of MB to the coatings is very small. On UV irradiation the concentration monotonically decreases with time due to photocatalytic bleaching. The bleaching rates, i.e., photocatalytic activities, of anatase nanocrystal-precipitated and hydrated titania nanosheet-precipited coatings are higher than that of the pure anatase coating. These results should be caused by the fact that there are larger effective surface areas for photocatalytic reaction in the anatase nanocrystal- and

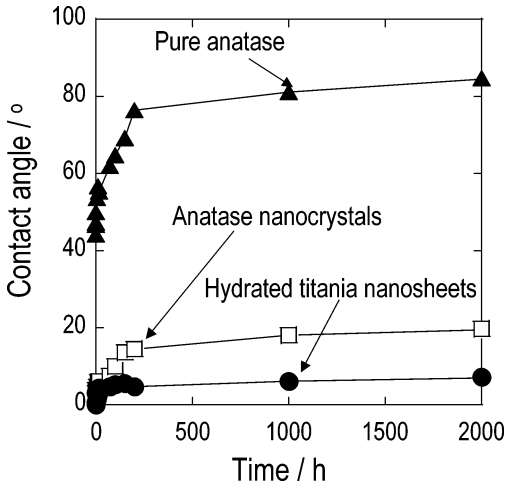

Figure 10. Changes in contact angle for water of the coatings during storage in the dark under ambient atmosphere. Open squares, closed circles, and closed triangles have the same meanings as in Figure 8.

hydrated tiatania nanosheet-precipitated coatings than in the pure anatase coating. This is presumed from the changes of morphology (shown in Figure 1) and the increases in surface roughness (shown in Figure 2) of the coatings. It is noteworthy that nanosheets of hydrated titania show a high photochatalytic activity comparable to that of anatase nanocrystals. When the anatase nanocrystal- and hydrated tiatania nanosheet-precipitated coatings are applied to the organic polymer substrates, the residual silica-rich underlayer of the coatings is expected to act as a protective layer for the substrates against the photocatalytic degradation. Therefore, this process is practically important to produce composition-gradient, multilayer, photocatalytic coatings at low temperatures.

Hydrophilicity of the coatings was examined from contact angles for water. Figure 9 shows changes in contact angle for water of the SiO_2-TiO_2 coatings during hot watertreatment. Open squares and closed circles represent the treatment conditions for anatase formation without vibration and for hydrated titania formation with a vibration at ca. 6 Hz, respectively. Before hot water treatment, contact angle for water of the coating was 60°. The contact angle decreases with treatment time under both conditions. This is caused by chemical and geometrical effects;[16] that is, the increase in surface energy due to the elimination of residual organic groups and the formation of very small roughness shown in Figures 1 and 2. When the coating is treated with hot water without vibration, the contact angle for water of the coating decreases to be minimized around 1−2 h and then slightly increases during the treatment. In comparison with the changes in surface roughness shown in Figure 2, the contact angle tends to level off over 2 h of the treatment. Thus the slight increase in contact angle implies the chemical property of the surface has changed. SiO_2 is well-known to show lower contact angel for water, i.e., higher surface energy, than TiO_2, so that the SiO_2-rich underlayer may become covered with anatase nanocrystals. On the other hand, as the coating is treated with hot water under vibration, the contact angle gradually decreases and becomes less than 5° over 5 h of treatment time, which corresponds to a monotone increase in surface roughness shown in Figure 2. The surface

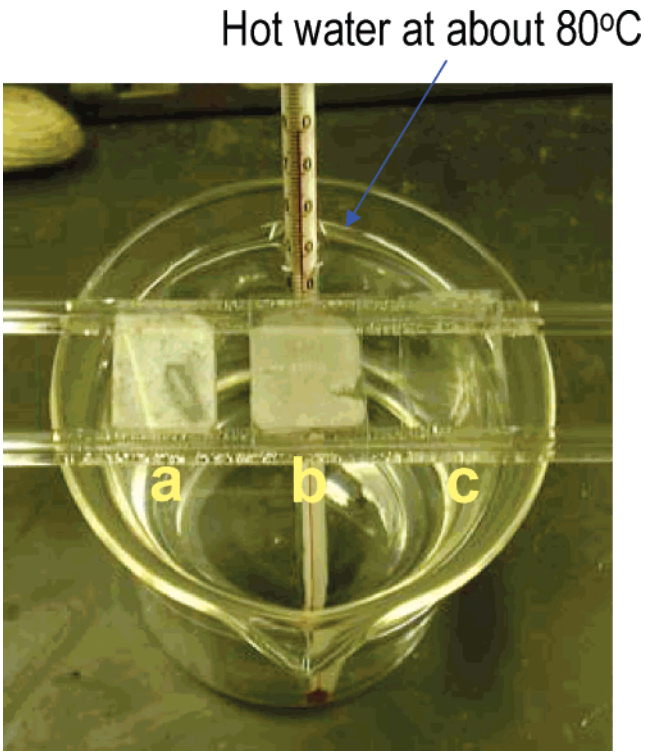

Figure 11. Photograph illustrating antifogging properties of the coatings holding over hot water at 80 °C in a beaker. (a), (b). and (c) are glass substrates with pure anatase coating, anatase nanocrystal-precipitated coating, and hydrated titania nanosheet-precipitated coating, respectively. This photograph was taken after the substrates with coatings were kept in a dark place and at ambient atmosphere for 2000 h.

of the underlayer is considered to be not yet wholly covered with titania nanosheets even after the treatment for 5 h. It can be seen that an excellent wettability, i.e. contact angles for water less than 5°, is achieved at around treatment time of 1−2 h without vibration and over 5 h under vibration.

Changes in contact angles for water of the coatings during storage in the dark under ambient atmosphere are shown in Figure 10. Open squares, closed circles, and closed triangles have the same meanings as in Figure 8. In the beginning of the storage, contact angles for water of the anatase nanocrystal- and hydrated titania nanosheet-precipitated coatings are less than 5°, while that of the pure anatase coating is about 40°. The contact angles of all the coatings increase with storage time because of the adsorption of organic substances in the atmosphere on the coatings as well as the structural changes of surface OH groups.[14] The hydrated titania nanosheet-precipitated coatings retain good hydrophilicity even after storage in the dark for 2000 h owing to the large roughness, unique morphology, and large surface energies of the hydrated titania and the silica-rich underlayer.[14] All the coatings were confirmed to show contact angles around 5° with UV irradiation after storage in the dark for 2000 h owing to the photocatalytic decomposition of organic adsorbates and photoinduced surface structural changes.

A photograph to demonstrate the antifogging properties of the coatings is provided in Figure 11. Three kinds of glass substrates with coatings, which were kept in the dark for 2000 h as described in Figure 10, were placed over hot water at 80 °C in a beaker. Samples a, b, and c correspond to pure anatase, anatase nanocrystal, and hydrated titania nanosheet coatings, respectively. Among the three kinds of coatings, c is seen to show the best antifogging property, indicating the hydrated titania nanosheet-precipitated coatings are versatile for applications in the field of optics as well as for photocatalysts.

Changes in the morphology as well as the crystalline phases of hydrated titania nanosheets with heat treatment are fundamentally important. Thus, the titania nanosheets heat-treated at various elevated temperatures were characterized using SEM, TEM, and electron diffraction. Sheetlike shape was retained even after a heat treatment at 600 °C, whereas the shape was partially changed to granular after a heat treatment at 700 °C. After a heat treatment at 1000 °C, sheetlike precipitates completely disappeared and only granular precipitates were observed. Lattice fringes of 0.6−0.8 nm on HRTEM and a ring pattern corresponding to 0.15

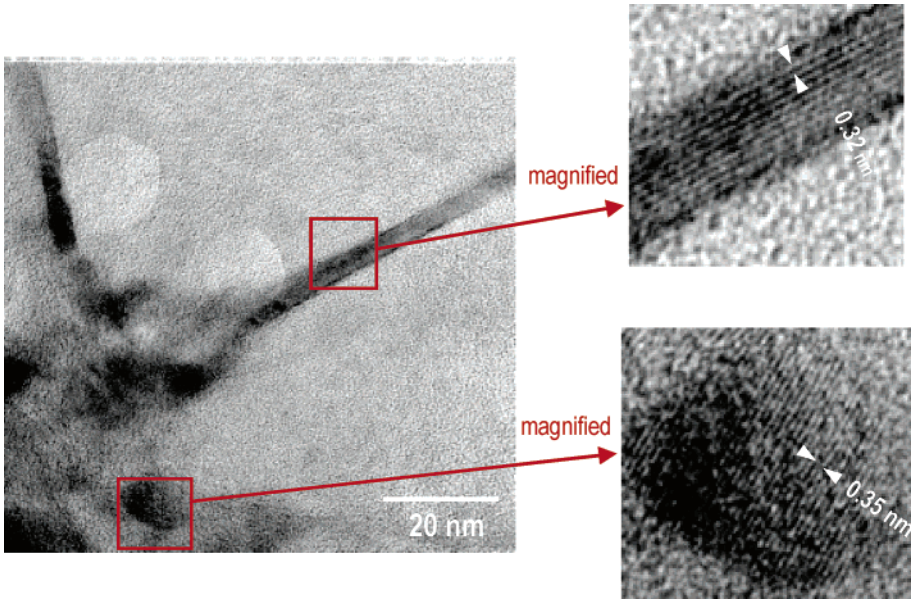

Figure 12. Plan-view TEM images of the coating heat-treated at 700 °C for 1 h. Bottom right is a granular nanocrystal with a spacing of 0.35 nm corresponding to (101) of anatase, and top right is a needlelike or platelike nanocrystal with a spacing of 0.32 nm corresponding to (110) of rutile.

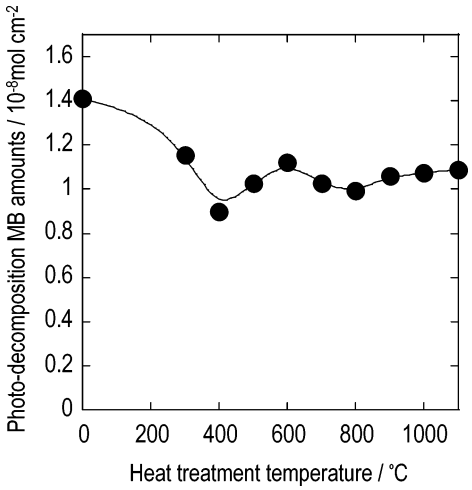

Figure 13. Amounts of MB photocatalytically decomposed by the titania-precipitated coatings during UV irradiation for 2 h. The coatings were obtained with hot water treatment under vibration at 6 Hz and then heated at various temperatures for 1 h.

nm spacing on electron diffraction were observed for the coating heat-treated at 500 °C, whereas both hydrated titania and anatase were observed for the coating heat-treated at 600 °C. Therefore, the hydrated titania nanosheet on the coating is thermally stable at around 500 °C. On the other hand, formation of platelike rutile and granular anatase were observed for the coating heat-treated at 700 °C. Typical plan-view TEM images of the coating heat-treated at 700 °C for 1 h are shown in Figure 12. The granular nanocrystals with a spacing of 0.35 nm corresponding to (101) of anatase are observed (bottom-right), whereas the needlelike or platelike nanocrystals have a spacing of 0.32 nm correspond to (110) of rutile (top right). This result suggests that hydrated titania nanosheets were transformed to rutile during the heat treatment. It is reported that hydrated titania is transformed to anatase at around 700 °C and to rutile at temperatures higher than 1000 °C.[26] Therefore, isolated nanosheet structure on the coating may permit the phase transition from anatase to rutile at lower temperatures.

Photocatalytic activities of the coatings heat-treated at various temperatures are notable. The amounts of MB photocatalytically decomposed by the coatings are compared in Figure 13. Heat treatment time was 1 h and the UV-irradiation time was 2 h for all the coatings. The amount of decomposed MB decreases with an increase in temperature up to 400 °C and then slightly increases at 600 °C, which should reflect the competition between a decrease in specific surface area and a formation of highly active anatase. It can be seen that the rutile-precipitated coatings heated at 1000 °C still show relatively high photocatalytic activities.

A practically important point is that the hydrated titania nanosheet-precipitated coatings can be formed at temperatures lower than 100 °C under atmospheric pressure. Consequently, this process has a great potential for applications to various substrates including organic polymers with poor heat resistance. Our work demonstrates that the crystalline phase and the morphology of nanocrystals-dispersed materials can be controlled in a relatively short time by treating sol−gel derived multicomponent gels with hot water under external dynamic conditions such as vibrations.

Conclusions

Unique coatings of titania nanosheet-precipitated coatings with high photocatalytic activity, excellent wettability for water, and antifogging properties have been prepared by treating sol−gel derived SiO_2-TiO_2 films with hot water at 90 °C under vibrations. Longitudinal vibrations with frequencies at around 6 Hz enhanced the formation of titania nanosheets during the treatment. The titania nanosheets mainly consisted of layers with a spacing of about 0.6 nm and were identified as hydrated titania with a lepidocrocite-type structure. The morphology of the titania nanosheet-precipitated coatings may be achieved by lowering the concentration of hydrolyzed titania species at the surface due to rapid water flow driven by the vibration. The hydrated titania nanosheet-precipitated coating maintained a very low contact angle for water and an antifogging property even after being kept in the dark for long time. The hydrated titania nanosheets were thermally stable up to 500 °C, and transformed to anatase at 600 °C and rutile at temperatures higher than 700 °C. This new approach developed here provides a promising route to dramatically modify the physicochemical properties and surface reactivity of nanocrystals-dispersed coatings.

Acknowledgment. This work was partly supported by Grant-in-Aid 15360344 (Section (B)) and 16360327 (Section (B)) for Scientific Research from the Ministry of Education, Culture, Sports, Science, and Technology of Japan and by Nippon Sheet Glass Foundation for Materials Science and Engineering, Tatematsu Foundation, Izumi Science and Technology Foundation, and Hosokawa Powder Technology Foundation.

CM048135H